Lowest excited states of ^{13}O

B. B. Skorodumov,[1,*] G. V. Rogachev,[2] P. Boutachkov,[1] A. Aprahamian,[1] V. Z. Goldberg,[3]
A. Mukhamedzhanov,[3] S. Almaraz,[1] H. Amro,[4] F. D. Becchetti,[4] S. Brown,[2,5] Y. Chen,[4]
H. Jiang,[4] J. J. Kolata,[1] L. O. Lamm,[1] M. Quinn,[1] and A. Woehr[1]

[1]*Institute for Structure and Nuclear Astrophysics, University of Notre Dame, Notre Dame, Indiana 46556, USA*
[2]*Physics Department, Florida State University, Tallahassee, Florida 32306, USA*
[3]*Texas A&M University, College Station, Texas 77843, USA*
[4]*Physics Department, University of Michigan, Ann Arbor, Michigan 48109, USA*
[5]*Department of Physics, University of Surrey, GU2 7XH, United Kingdom*

An excitation function for resonance elastic scattering of $p + {}^{12}$N was measured in the center of mass energy range of 0.8–2.7 MeV. Measurements were performed using inverse kinematics and the thick-target techniques. The data were analyzed in the framework of the **R**-matrix formalism. A definitive spin and parity assignment was possible for the first excited state of ^{13}O at an excitation energy of 2.69 MeV as $J^\pi = \frac{1}{2}^+$. An indication of the presence of a new level in ^{13}O at an excitation energy of 3.29 MeV with tentative spin-parity assignment $J^\pi = \frac{1}{2}^-$ or $\frac{3}{2}^-$ was obtained. We evaluate the impact of this measurement on the reaction rate of ^{12}N$(p,\gamma)^{13}$O for nucleosynthesis in low-metallicity stars.

PACS number(s): 21.10.−k, 24.30.−v, 27.20.+n

I. INTRODUCTION

The level schemes of the $A = 13$, $T = 3/2$ nuclei are sparse due to experimental difficulties in reaching them in conventional nuclear reactions. Although some excited states have been identified in ^{13}B, mainly using the ^{11}B(t,p) reaction [1] (Fig. 1), there exists no definite knowledge about their quantum characteristics and hence no knowledge about their structure. A few excited states have been found in ^{13}O using the ^{13}C$(\pi^+, \pi^-)^{13}$O double charge exchange reaction. Among these, the lowest had an assigned excitation energy of 2.75 ± 0.04 MeV [2]. A state at a similar excitation energy $(2.82 \pm 0.24$ MeV$)$ was observed in the ^{12}C$(p,\pi^-)^{13}$O reaction [3]. All these data were obtained with an energy resolution of $\sim$0.5 MeV and limited statistics, resulting in no definite quantum characteristics for the observed states. Figure 1 shows that all excited states of ^{13}O are unstable with respect to proton decay to the ground state of ^{12}N. There is a large shift of the first excited state in ^{13}O, in comparison with the level spacing in ^{13}B. This large shift might be related to the Thomas-Ehrman effect [4] for s states. The structure of this state can be probed in resonance elastic scattering of radioactive ^{12}N on hydrogen, previously studied by Teranishi *et al.* [5] at zero degrees. However, no analysis was presented in that article.

The nuclear structure of ^{13}O is important for the evolution of very low-metallicity massive stars. In 1989 Wiescher, Buchmann, and Thielemann [6] suggested several reaction sequences that would permit very massive stars with low-metallicity to bypass the 3α process. They determined the required temperature and density conditions where capture reactions on short-lived nuclei were of equal strength to competing β decays or inverse photodisintegration. They found that the ^{3}He$(\alpha, \gamma)^7$Be$(\alpha, \gamma)^{11}$C reactions could represent an

important path from helium to carbon isotopes. The ^{11}C produced in this sequence may decay and return to ^{4}He via ^{11}C$(\beta^+, \nu)^{11}$B$(p,\alpha)^8$Be$(^4$He,^{4}He$)$ or be depleted by proton capture into the $A > 12$ region through ^{11}C$(p,\gamma)^{12}$N. ^{12}N can be depleted into ^{12}C through β^+ decay or by photodisintegration $(^{12}$N$(\gamma,p)^{11}$C$)$. However, ^{12}N may also capture a proton to form ^{13}O through the process ^{12}N$(p,\gamma)^{13}$O. This process can compete with β^+ decay and photodisintegration of ^{12}N at some temperatures and densities. It is important to evaluate the density and temperature regime where this may occur.

In this work, the excitation function for resonance elastic scattering of ^{12}N$+p$ was measured at several scattering angles. The spin-parity, width, and excitation energy of the first excited state of ^{13}O were determined. An indication of the presence of a second excited state at 3.29 MeV, with quantum characteristics $1/2^-$ or $3/2^-$, was obtained. We also examine the impact of this new experimental information on the ^{12}N$(p,\gamma)^{13}$O reaction that might play an important role in nucleosynthesis in low-metallicity stars.

II. EXPERIMENT

The elastic scattering of a radioactive ^{12}N beam on protons was performed at ISNAP (Institute for Structure and Nuclear Astrophysics) at the University of Notre Dame using the TwinSol radioactive ion beam facility Ref. [7,8]. A primary 43 MeV ^{10}B beam with an intensity of 30 pnA was focused onto a 2.5-cm-long gas cell filled with ^{3}He at a constant pressure of 1.3 atm. The secondary ^{12}N radioactive beam (half-life 11 ms) was produced via the ^{10}B$(^3$He,$n)^{12}$N reaction. The outgoing reaction products were captured in the angular region from $2°$ to $5°$ by TwinSol. The two superconducting solenoids of TwinSol act as thick lenses to separate the ^{12}N beam from other reaction products. The magnetic rigidity of the first solenoid was set to focus ^{12}N^{6+} ions onto a 10 μg/cm^2
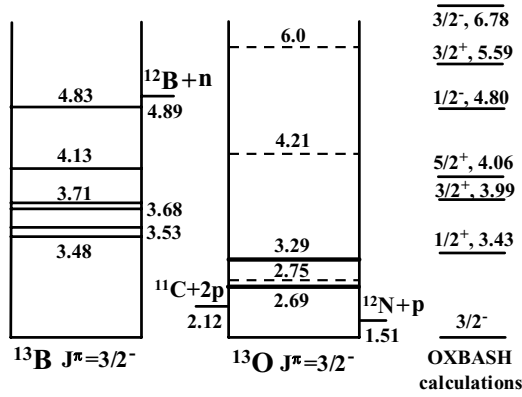
FIG. 1. Level scheme of the mirror nuclei ^{13}B and ^{13}O. The dashed lines in the ^{13}O level scheme represent levels from Ref. [1]. The solid lines are the present results. On the right side of the figure, OXBASH calculations [11] with the WBT [12] interaction are presented.

FIG. 3. The spectra of protons observed from a polyethylene target and a natural carbon target in a Si detector at 7.5° in the laboratory frame. The hashed histogram shows a proton spectrum from the natural carbon background; the solid line shows the polynomial fit that was used to subtract the carbon background.

stripping foil. The second solenoid focused fully stripped ^{12}N^{7+} ions onto the secondary polyethylene (CH$_2$) target in a 1 cm diameter spot. Under these conditions, a ^{12}N beam of 10^3 pps having an energy of 46 MeV and an energy spread of 1.8 MeV full width at half maximum (FWHM) was obtained. The desired ^{12}N ions made up only 7% of the secondary beam; the main contamination was ^{10}B (Fig. 2). The thickness of the polyethylene (CH$_2$) secondary target was 8.2 mg/cm^2 to stop the ^{12}N ions. Three Si ΔE-E detectors placed at angles of 7.5°, 22.5°, and 37.5° with respect to the beam axis were used to detect recoil protons. Because the primary ^{10}B beam was pulsed with a repetition rate of 5 MHz and a pulse width of approximately 2 ns, the 5.6 m distance from the primary target to the array of silicon detectors was adequate to obtain a clean separation of the protons associated with the interaction of ^{12}N ions in the target from protons associated with elastic scattering or reactions of beam contaminants. A measurement with a natural carbon target was also performed to enable subtraction of events relevant to the presence of carbon in
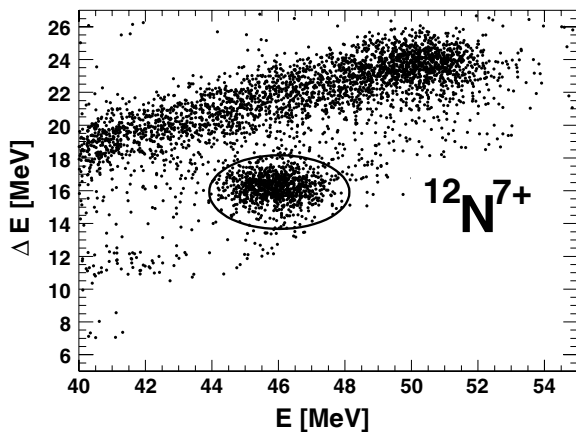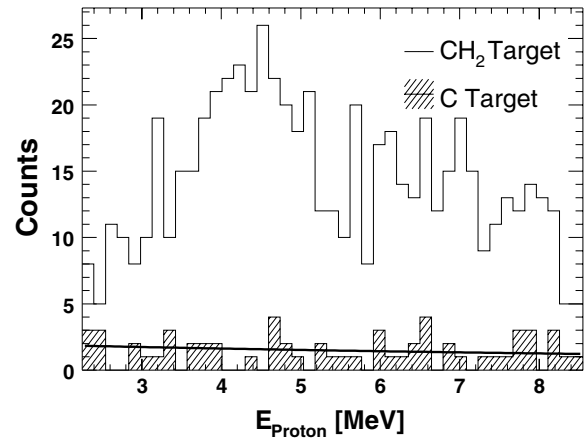
the polyethylene target (see Fig. 3). The excitation functions were transformed to the center-of-momentum system on a bin-by-bin basis, using a computer code that takes into account kinematics, geometry of the experimental setup, specific energy losses for ^{12}N and protons, and the total number of accumulated ^{12}B ions.

III. RESULTS AND DISCUSSIONS

The experimental excitation functions, converted into the center-of-momentum system, are shown in Figs. 4 and 5 together with an **R**-matrix fit. Figure 4 shows the excitation function with a single-resonance fit. This does not resemble the spectrum expected from several tightly spaced levels as seen in ^{13}B. Primarily, this is because the $l = 0$ resonance is shifted down in excitation energy relative to the other levels due to the Thomas-Ehrman effect [4]. Indeed, the shape of the resonance

FIG. 2. Two-dimensional picture from a ΔE-E Si telescope placed at the secondary target position. The major contaminant (^{10}B^{5+}) is off scale at a total energy of 28 MeV. "Pileup" events from this group are clearly seen.
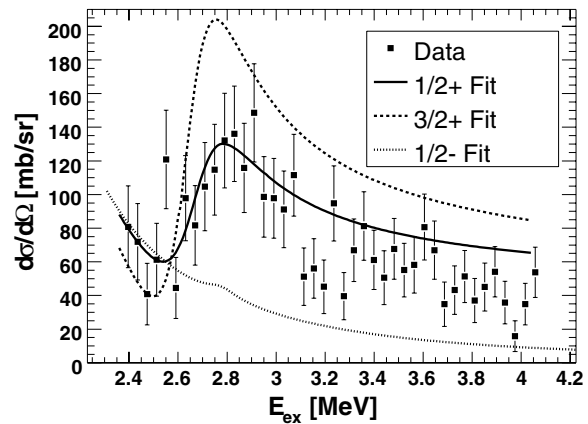

FIG. 4. Single-resonance **R**-matrix fits for the experimental data from the detector at 7.5°. The solid line shows the fit with the assumption of a single $1/2^+$ resonance. A $3/2^+$ assignment would lead to the fit shown by the dashed line. A $1/2^-$ assignment would lead to the fit shown by dotted curve.

as well as the gross structure of the excitation function (Fig. 4) is described by a single $l = 0$ resonance. All other possibilities are easily rejected on the basis of shape and width considerations, as shown in Fig. 4 for an $l = 1$ resonance. Two spin values, $1/2^+$ and $3/2^+$, can be obtained as a result of the coupling of the ^{12}N ground-state spin, 1^+, to that of an $l = 0$ proton. As can be seen in Fig. 4, the calculated cross section for the $3/2^+$ assignment greatly exceeds the experimental value. In these calculations, we took into account only one (proton) channel for the decay of the resonances. The $2p$ decay to the ^{11}C ground state is also possible (Fig. 1). However, due to unfavorable penetrability, this decay route is at least 1000 times less probable than one-proton decay. Therefore it can be concluded that the single-resonance approach rules out a $3/2^+$ resonance and favors a $1/2^+$ assignment for this state.

However, this conclusion could be changed if distant resonances are included and only the absolute cross section is considered. In addition to the theoretical predictions and existing data for the ^{13}B spectra, one can find some direct indications for the presence of additional resonances in Fig. 4. There is a small dip at 3.29 MeV, and a disagreement between the calculations and the experimental data in the high-energy part of the excitation function. A more detailed analysis of the excitation functions is presented below. However, it is worthwhile noting that the single level approximation, as well as the more sophisticated analysis, both give a very precise excitation energy for the $1/2^+$ resonance, $E_{\text{ex}} = 2.69 \pm 0.05$ MeV, whereas the resonance width Γ could not be defined with high precision in the present experiment.

Figure 5 shows the best **R**-matrix fit to the experimental excitation functions. The calculations include, in addition to the $l = 0$ resonance, a narrow $1/2^-$ resonance at 3.29 MeV excitation energy and three distant resonances $(3/2^-, 3/2^+, 3/2^+)$. The resonance parameters are tabulated in Table I. The parameters of the distant resonances were chosen in agreement with OXBASH calculations [11,12] performed in an s-p-sd-pf valence space with the WBT interaction, with only $0\hbar\omega$ and $1\hbar\omega$ excitations allowed. We did not, however, use the excitation energies calculated in Ref. [11,12] because: (1) the calculations were not made for unbound states and (2) the precision of OXBASH predictions is generally not better than 1.0 MeV in the region of interest. We also did not try to fit the excitation energies of the two known states in ^{13}O at 4.3 and 6.0 MeV because the quantum characteristics of these levels are not known. Although two of the three distant levels appear to be close to the above-mentioned values, this may be accidental. The main aim of including the resonances

FIG. 5. **R**-matrix fits to the excitation functions. The solid curves represent the best fit for a $1/2^+$ assignment to the resonance at 2.69 MeV. The other parameters are given in Table I. The dashed curve (top panel) is the same except for resonance spin $3/2^+$ and a width of 200 keV. The dotted curve is a similar calculation except that the $3/2^+$ resonance has a width of 400 keV. All calculations also include a $1/2^-$ resonance at 3.29 MeV.

in question was to understand their influence on the region of interest. Each of these levels, both separately and together, influence the calculated cross section in the high energy part of the excitation function in a similar way, toward better agreement with the experiment. We found that this feature is preserved when we change the excitation energies of the levels over a broad region. We also found that, if the first $3/2^+$ resonance is located within the energy region of our measurements, it would produce obvious disagreement with the measured excitation function. However, the presence of the second $3/2^+$ level is necessary as it yields a flat region at higher excitation energy in agreement with the experimental data.

The dip at 3.29 MeV excitation energy can be fitted by an $l = 1$ resonance. (Other possibilities were tested and rejected after inspection of the predicted shape and width.) The coupling of the orbital angular momentum and spins of ^{12}N and the proton would yield a resonance spin of $1/2^-$, $3/2^-$, or $5/2^-$. All these spins result in a similar shape for the resonance but yield different cross sections. The $5/2^-$ assignment can be rejected on the basis of cross-section considerations. The fit is better for the $1/2^-$ assignment than for $3/2^-$. However, the present data do not allow for a reliable selection between these

TABLE I. Resonance parameters for levels in ^{13}O.

N	J^π	E_{ex} MeV	Γ MeV
1	$1/2^+$	2.69 ± 0.05	0.45 ± 0.1
2	$(1/2,3/2)^-$	3.29 ± 0.05	0.075 ± 0.03
3	$(3/2^-)$[a]	(4.55)	(0.24)
4	$(3/2^+)$[a]	(5.00)	(0.78)
5	$(3/2^+)$[a]	(5.70)	(2.00)

[a]Distant resonances used in the **R**-matrix fit.

two possible spin assignments. Inclusion of the $\ell = 1$ state at 3.29 MeV improves the χ^2 from 1.39 to 0.82.

Fixing the parameters of the weaker resonances, we next tried to find the best-fit parameters for the $l = 0$ resonance. As can be seen in Fig. 5 (top), the $3/2^+$ assignment results in a cross section that is too large. A somewhat better fit can be obtained for a $3/2^+$ resonance with a narrower width (200 keV). However, as shown below, the narrow width is in contradiction with the excitation energy of the resonance. The best fit parameters ($\chi^2 = 0.8$) of the $1/2^+$ resonance are 2.69 MeV for the excitation energy and 450 keV for the width. Unfortunately, the χ^2 dependence is very flat, giving a width ranging from 0.35 to 0.55 MeV.

A more detailed insight into the level structure of ^{13}O can be derived using a potential-model approach with isobaric shift considerations. As can be seen from Fig. 1, four lowest (closely spaced) excited levels have been found at an excitation energy of ~ 3.5 MeV in ^{13}B. Although the spins of these levels are not known, the authors of Ref. [1] claim that the spin of the lowest of these four states at 3.48 MeV could be $1/2^+$, $3/2^+$, or $5/2^+$ and that the spin of the state at 3.53 MeV could be $1/2^-$, $3/2^-$, or $5/2^-$.

The excitation energies of the s states should be strongly shifted down in ^{13}O relative to their positions in ^{13}B due to the Thomas-Ehrman effect [4]. Two sets of Woods-Saxon potentials were used to calculate this shift for a pure $2s_{1/2}$ single-particle state. The first one was rather conventional (Table II, first row). The other one was taken in agreement with the recommendation in Ref. [13] (Table II, second row). In both cases, the well depth was chosen to fit the excitation energy of the lowest excited state in ^{13}B. The results of these potential-model calculations are summarized in Table II. Both parameter sets give similar values for the shift, ~ 1 MeV. Thus, the predicted position of the $\ell = 0$ single-particle resonance in ^{13}O is 2.4–2.5 MeV. (It was verified that the positions and widths of the calculated single-particle resonances are insensitive to Coulomb radius variations in the region from $r_{\mathrm{Coul.}} = 0.7$ to 1.2 fm.) Evidently, the shift of the specific state is proportional to the single-particle spectroscopic factor. Simple considerations lead to the conclusion that the $1/2^+$ level has a larger single-particle spectroscopic factor than the $3/2^+$ state. Indeed, due to the sign of the spin-orbit interaction, the $d_{5/2}$ configuration is close to the $2s_{1/2}$ state. With a core spin equal to 1^+, the $d_{5/2}$ configuration cannot contribute to a $1/2^+$ state, whereas it can directly contribute to $3/2^+$ states. (There is a small probability for contributions from

TABLE II. Potential-model results for the $1/2^+$ state in ^{13}O.

V_0 MeV	r_0[a] fm	a fm	Γ_{sp} MeV	Δ[b] keV	ε (MeV) Isotopic shift	S_f[c]
-56.60	1.22	0.600	525	0.16	0.65	0.77
-56.65	1.17	0.735	717	0.29	0.74	0.60

[a]$r_{\mathrm{Coul.}} = 1.21$ fm.
[b]$\Delta = E_{\mathrm{res}} - E_{\mathrm{sp}}$.
[c]$S_f = 1 - \Delta/\varepsilon$.

the $d_{5/2}$ single-particle configuration to the $1/2^+$ state via 2^+ core excitation). OXBASH shell-model calculations confirm the simple considerations above. They predict one low-lying $1/2^+$ state with a single-particle spectroscopic factor of 0.67 and two $3/2^+$ states (see Fig. 1) lying above the $1/2^+$ state and having $2s_{1/2}$ spectroscopic factors equal to 0.27 and 0.44, respectively. Therefore, the $1/2^+$ state in ^{13}O should be shifted down relative to the $3/2^+$ state by several hundred keV, in agreement with our $1/2^+$ assignment for the first excited state of ^{13}O.

Referring to Table II, a pure single-particle level would be ~ 300 keV lower than the experimental excitation energy of 2.69 MeV. This leaves room for a more complicated structure for the $1/2^+$ state in ^{13}O. To obtain the correct excitation energy, the single-particle spectroscopic factor for this state would be 0.60–0.77 (the lower value corresponds to the more diffuse potential). Using the data from Table II, one can obtain the corresponding widths for an s state at 2.69 MeV. These are 440 keV for the "conventional" potential and 507 keV for the "diffuse" potential. These values provide an additional reason to exclude the fits based on the assumption that the lowest excited state in ^{13}O is a narrow $3/2^+$ state. It seems important to note that more exact experimental data on the width of this state would be decisive for the choice of a potential to describe the single-particle states of drip-line nuclei in this region. At present we note that the spectroscopic factor corresponding to the diffuse potential is closer to the OXBASH prediction of $S_f = 0.67$.

Continuing these considerations, one can relate the $(1/2, 3/2)^-$ state in ^{13}O to the second excited state in ^{13}B. The ~ 200 keV shift in the excitation energy of these states can be explained as a manifestation of the "pure" Thomas-Ehrman effect [4] for $\ell = 1$ state (this state is bound against particle decay in ^{13}B but unbound in ^{13}O).

IV. ASTROPHYSICAL S FACTOR AND REACTION RATES FOR THE ^{12}N$(p, \gamma)^{13}$O RADIATIVE CAPTURE

The first estimate of the reaction rate and astrophysical S-factor for ^{12}N$(p,\gamma)^{13}$O radiative capture was carried out in Ref. [6], where it was assumed that the reaction proceeds through the $3/2^+$ resonance at an excitation energy of $E_x = 2.75$ MeV via direct $E1$ capture to the ground state of ^{13}O. The radiative width of the first resonance was assumed to be 24 meV. The proton partial width of the resonance was not available at that time. The astrophysical factor for direct radiative capture was also estimated but the interference between the direct and resonance terms was not taken into account [6].

The new experimental data on the first excited state in ^{13}O prompt a re-evaluation of the ^{12}N(p,γ) reaction rate. Calculations have been performed within the framework of the **R**-matrix method using the equations given in Refs. [14,15]. The direct proton $s \to p$ $E1$ capture to the ground state in ^{12}N$(p,\gamma)^{13}$O is predominantly peripheral due to the small proton binding energy of the ground state: $\varepsilon = 1.51$ MeV. Therefore, the overall normalization of the direct

capture amplitude is entirely determined by the asymptotic normalization coefficient (ANC) for the virtual synthesis ^{12}N $+ p \rightarrow$ ^{13}O. Unfortunately this ANC is not yet available. For a more accurate estimation of the direct and total astrophysical factors for ^{12}N$(p,\gamma)^{13}$O, it is imperative to determine the proton ANC for the ground state of ^{13}O.

In this work the ^{13}O ground state ANC was estimated using the following approach. The single-particle spectroscopic factor for the ^{13}O ground state was calculated using the shell-model code OXBASH, which produces a spectroscopic factor $S_f \approx 0.7$ for $p + {}^{12}$N with $\ell = 1$ and the channel spin $I = 1/2$ configuration of the ground state of ^{13}O. A spectroscopic factor $S_f = 0.75$ was adopted. The single-particle $p + {}^{12}$N wave function was then calculated, using a Woods-Saxon potential with geometrical parameters $r_0 = 1.20$ fm and $a = 0.65$ fm, with the depth adjusted to reproduce the experimental proton binding energy. The single-particle ANC (the amplitude of the tail of the proton bound state wave function divided by the Whittaker function) for these parameters is $b = 2.14$ fm^{-1}. Correspondingly, the ANC for ^{12}N $+ p \rightarrow$ ^{13}O is $C = bS_f^{1/2} = 1.85$ fm^{-1}. Note that due to the small proton binding energy variation of the bound state potential geometrical parameters do not change the ANC significantly. For example, for $r_0 = 1.30$ fm and $a = 0.65$ fm the single-particle ANC is $b = 2.27$ fm^{-1} and $C = 1.96$. Another missing ingredient in the calculation of the proton-capture amplitude is the resonance radiative width Γ_γ. The radiative width $\Gamma_\gamma \sim |M_\gamma|^2$ from the dipole matrix element is given by

$$M_\gamma = \langle \varphi_{\mathrm{gs}} | \hat{O} | \psi_{1/2^+} \rangle, \qquad (1)$$

where $\psi_{1/2^+}$ is the ^{13}O$(1/2^+)$ resonance wave function, φ_{gs} is the wave function of the ground state of ^{13}O and $\hat{O}$ is the dipole electromagnetic operator. Two different approaches were used to estimate it. In the first approach, the shell model was used to calculate the wave functions and the matrix element. A value of 2.3 eV was obtained Ref. [17] (assuming that the radius of ^{13}O is 2.8 fm). In the second model, a standard **R**-matrix approach was used in which the dipole matrix element can be split into internal and external parts [14–16]:

$$M_\gamma = M_{\gamma(<)} + M_{\gamma(>)}. \qquad (2)$$

Here $M_{\gamma(<)}$ is the internal matrix element contributed by the radial integral taken over the nuclear interior ($r < R$), where R is the channel radius:

$$M_{\gamma(<)} = S_f^{1/2} |\langle \varphi_{\mathrm{gs}}(r) || r || \psi_{1/2^+}(r) \rangle|_{r<R}. \qquad (3)$$

The channel (or external) matrix element is determined by the radial integral taken over the nuclear exterior, $r > R$, where the wave functions can be replaced by their asymptotic values:

$$M_{\gamma(>)} = C \left| \left\langle \frac{W(r)}{r} || r || \psi_{1/2^+}(r) \right\rangle \right|_{r>R}. \qquad (4)$$

Here C is the ANC for the ^{13}O $\rightarrow$ ^{12}N $+ p$, $W(r)$ is the Whittaker function determining the tail of the proton bound-state wave function in ^{13}O. We note that $\Gamma_\gamma \sim |M_{\gamma(<)} + M_{\gamma(>)}|^2$ is the total radiative width. Also S_f is the spectroscopic factor of the configuration ^{12}N $+ p$ in the ground state of ^{13}O. The

internal part is model dependent. It was estimated using the single-particle ^{13}O $\rightarrow$ ^{12}N $+ p$ model. The channel part is model-independent because it is contributed by the asymptotic terms of the wave functions. The leading asymptotic term of the resonant wave function is also well known. The asymptotic behavior of the radial bound-state wave function is given by $S_f^{1/2} \varphi_{\mathrm{gs}}(r) \approx C W(r)/r$, where C is the proton removal ANC of the ground state of ^{13}O and W is the Whittaker function. Hence, the overall normalization of the channel part of the matrix element is governed by the ANC, and we can quite accurately estimate the external part of the matrix element. We find that the dominant contribution to the matrix element comes from the external matrix element, hence the sensitivity to the internal contribution is significantly diminished. The calculated total radiative width is $\Gamma_\gamma \approx 3$ eV for the channel radius $R = 4.25$ fm. To check the sensitivity of the radiative width to the model parameters, the channel radius and spectroscopic factor were varied. We find that $\Gamma_\gamma = 2.63$ eV for $R = 4.5$ fm and $S_f = 0.675$ and $\Gamma_\gamma = 3.32$ eV for $R = 4.0$ fm and $S_f = 0.825$. The adopted value was $\Gamma_\gamma = 3.00$ eV for $R = 4.25$ fm and $S_f = 0.75$. Because the ANC has a very small uncertainty this estimation of the radiative width is quite accurate. We believe that the slightly higher result obtained in the second method is related to the different asymptotic behavior of the shell-model wave function compared with the correct asymptotic terms used in the second method. Both methods give a radiative width that is significantly larger than the 24 meV used in Ref. [6].

The astrophysical S factor for the radiative capture ^{12}N$(p, \gamma)^{13}$O is dominated by the resonant capture to the ground state proceeding through the first $1/2^+$ resonance and by direct capture to the ground state. The amplitudes of the resonant and direct captures do interfere. Due to the small proton binding energy in the ground state of ^{13}O, the direct capture amplitude is entirely peripheral and its sign is determined by the ANC [15,16]. The resonant radiative capture amplitude can be split into internal and channel (external) parts. The sign of the external part is determined by the sign of $M_{\gamma(>)}$, i.e., by the ANC. Hence the relative sign of the resonant channel amplitude and the direct capture amplitude is well determined and it is positive for the case under consideration, for energies below the first resonance. The sign of the internal part is not known and can be determined only from microscopic-model calculations. However, the contribution from the internal part is smaller than that of the channel part due to the node in the resonant wave function. As a result, the total interference pattern is entirely determined by the interference of the resonant channel and direct capture amplitudes, which is constructive at energies below the first resonance [15,16].

The results of the calculation of the astrophysical factor and reaction rates are shown in Figs. 6 and 7. To determine the uncertainty of the calculated astrophysical factor we varied the channel radius from $R = 4.0$ fm to $R = 4.5$ fm with the adopted value of $R = 4.25$ fm. The spectroscopic factor varied from $S_f = 0.675$ to $S_f = 0.825$ with the adopted value $S_f = 0.75$.

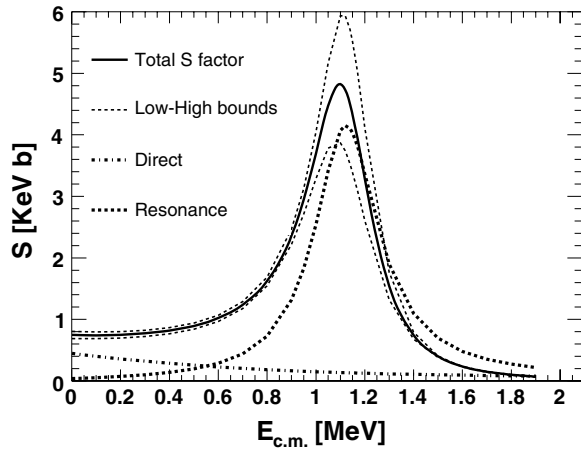The astrophysical reaction rates for the coherent sum of nonresonant capture and the first resonance was calculated

FIG. 6. The *S* factor calculations: the solid line shows accepted *S* factor; the region between two solid dashed lines show the upper and low limits of the calculated *S* factor obtained by variation of the channel radius and the spectroscopic factor; the dashed line shows only resonance capture contribution; the dashed-dotted line shows only direct capture contribution.

in the formalism presented in Ref. [15]. Our revised reaction rate for $^{12}\text{N}(p,\gamma)^{13}\text{O}$ implies that it will compete successfully with β^+ decay at lower densities than previously believed. Figure 7 shows the temperature regime of the former [6] and present calculations.

V. SUMMARY

In summary, we found that the first excited state of ^{13}O is at an excitation energy of 2.69 ± 0.05 MeV and has a width of 350–550 keV. We assigned a spin-parity of $1/2^+$ to this state on the basis of the shape of the resonance, the absolute value of the cross section, and the strong isotopic shift. The experimental data suggest a second excited state in ^{13}O at 3.29 ± 0.05 MeV with a tentative spin-parity assignment of $1/2^-$ or $3/2^-$ and a width of $\sim$75 keV. Another measurement with higher statistics is required to verify this result. Shell-model calculations [18] lead to the conclusion that
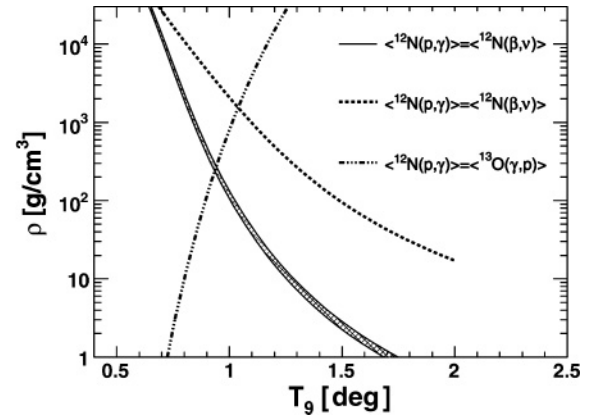

FIG. 7. The temperature and density conditions where the $^{12}\text{N}(p,\gamma)$ reaction is important. The region between two solid line (new results with uncertainty) and dashed line (from Ref. [6]) show where the rates for ^{12}N proton capture and beta decay of ^{12}N will be equal. In addition, the density should be above the dashed-dotted line to produce ^{13}O faster than it can be photo-dissociated.

the negative-parity states ($1/2^-$, $3/2^-$) in ^{13}B should occur at an excitation energy of around 4 MeV. The state we observed at 3.29 MeV may well be the mirror of one of these levels. An important role in the descent of the $1/2^+$ state could be played by a diffuse nuclear potential, which makes the state broader as well. More exact measurements of the width of the $1/2^+$ state will be important for making a choice between conventional and diffuse potentials in the description of single-particle states in light drip-line nuclei. Our revised reaction rate for $^{12}\text{N}(p,\gamma)^{13}\text{O}$ implies that it will compete with β^+ decay and photodisintegration of ^{12}N at stellar densities lower than previously believed.

[1] F. Ajzenberg-Selove, Nucl. Phys. **A449**, 1 (1986).
[2] P. A. Seidl *et al.*, Phys. Rev. C **30**, 1076 (1984).
[3] P. Couvert *et al.*, Phys. Rev. Lett. **41**, 530 (1978).
[4] J. B. Ehrman, Phys. Rev. **81**, 412 (1951); R. J. Thomas, Phys. Rev. **88**, 1109 (1952).
[5] T. Teranishi *et al.*, Nucl. Phys. **A718**, 207 (2003).
[6] M. Wiescher, J. Górres, S. Graff, L. Buchmann, and F.-K. Thielemann, Astrophys. J. **343**, 352 (1989).
[7] M.-Y. Lee, Ph.D. thesis, University of Michigan (2002).
[8] M.-Y. Lee *et al.*, Nucl. Instrum. Methods Phys. Res., Sect. A **422**, 536 (1999).
[9] J. Ziegler, http://www.srim.org (2003).
[10] A. M. Lane and R. G. Thomas, Rev. Mod. Phys. **30**, 257 (1958).

[11] B. A. Brown, A. Etchegoyen, and W. D. M. Rae, MSU-NSCL Report No. **524** (1986).
[12] E. K. Warburton and B. A. Brown, Phys. Rev. C **46**, 923 (1992).
[13] V. Z. Goldberg, G. G. Chubarian, G. Tabacaru, L. Trache, R. E. Tribble, A. Aprahamian, G. V. Rogachev, B. B. Skorodumov, and X. D. Tang, Phys. Rev. C **69**, 031302(R) (2004).
[14] F. C. Barker and T. Kajino, Astrophys. J. **44**, 336 (1991).
[15] X. Tang *et al.*, Phys. Rev. C **67**, 015804 (2003).
[16] X. Tang *et al.*, Phys. Rev. C **69**, 055807 (2004).
[17] A. Volya (private communication), 2006.
[18] A. A. Wolters, A. G. M. van Hees, and P. W. M. Glaudemans, Phys. Rev. C **42**, 2062 (1990).